DALTON
FULL PAPER

Platinum group metal complexes of arylphosphine ligands containing perfluoroalkyl ponytails; crystal structures of [$RhCl_2(\eta^5-C_5Me_5)\{P(C_6H_4C_6F_{13}-4)_3\}$] and *cis*- and *trans*-[$PtCl_2\{P(C_6H_4C_6F_{13}-4)_3\}_2$]

John Fawcett, Eric G. Hope,* Raymond D. W. Kemmitt, Danny R. Paige, David R. Russell and Alison M. Stuart

Department of Chemistry, University of Leicester, Leicester, UK LE1 7RH

Received 3rd July 1998, Accepted 23rd September 1998

The triarylphosphine ligands $PPh_{3-x}(C_6H_4C_6F_{13}-4)_x$, $x = 1$, 2 or 3, reacted with [$\{RhCl_2(\eta^5-C_5Me_5)\}_2$], [$\{RhCl(CO)_2\}_2$], [{IrCl(COD)}$_2$], [$PdCl_2(MeCN)_2$] or [$PtCl_2(MeCN)_2$] to yield the complexes [$RhCl_2(\eta^5-C_5Me_5)L$] **1**–**3**, *trans*-[$RhCl(CO)L_2$] **4**–**6**, *trans*-[$IrCl(CO)L_2$] **7**–**9**, *trans*-[$PdCl_2L_2$] **11**–**13** or *cis*-/*trans*-[$PtCl_2L_2$] **14**–**16** respectively. Spectroscopic studies and structural studies (EXAFS for **4**–**9**, **11**–**15** and X-ray single crystal for **3** and **16**) indicated that the aryl groups are fairly good insulators of the electronic influence of the perfluoroalkyl substituents whilst solubility studies indicated that at least six C_6F_{13} units are necessary for preferential perfluorocarbon solvent solubility and that the type of metal complex is important, *i.e.* the Vaska's analogues **6** and **9** are perfluorocarbon solvent soluble whereas the dichloride complexes **13** and **16** are not. Studies on the addition of dioxygen to **7**–**10** identified a stepwise reduction in rate following the introduction of the perfluoroalkyl ponytails.

One of the important areas of development in homogeneous catalysis is improvements in catalyst/product separation and catalyst recycling. Recently, the fluorous (perfluoroalkyl) biphase system (FBS) was proposed as a new approach.[1] This entails anchoring a catalyst in a perfluorinated solvent by the attachment of long, perfluorinated, aliphatic side-chains (called fluorous "ponytails") and product/catalyst separation arises from the immiscibility of many conventional organic and perfluorinated solvents. This approach has now been adopted in a series of homogeneous catalysis processes.[1–6] Recently, we reported the preparations of a range of related perfluoroalkyl-derivatised phosphorus(III) ligands[7] and here describe the co-ordination chemistry of analogues of triphenylphosphine with 1, 2 or 3 ponytails with a range of platinum group metals, including the structure of a highly unusual mixture of *cis*- and *trans*-[$PtCl_2L_2$] complexes, to assess the influence of these fluorous ponytails on the co-ordination, reactivity and solubility properties of metal complexes.

Experimental

Proton, ^{19}F and ^{31}P NMR spectroscopies were carried out on a Bruker ARX250 spectrometer at 250.13, 235.34 and 101.26 MHz or a Bruker DRX 400 spectrometer at 400.13, 376.50 and 161.98 MHz and were referenced to external $SiMe_4$ (^1H), to external $CFCl_3$ (^{19}F) and to external 85% H_3PO_4 (^{31}P) using the high-frequency positive convention. The IR spectra were recorded on a Digilab FTS40 Fourier-transform spectrometer at 4 cm^{-1} resolution for the complexes as Nujol mulls held between KBr discs or for solutions in $CHCl_3$ held between KBr plates. Elemental analyses were performed by Butterworth Laboratories Ltd.. Mass spectra were recorded on a Kratos Concept 1H mass spectrometer. Rhodium and palladium K-edge and iridium and platinum L_{III}-edge EXAFS data were collected at the Daresbury Synchrotron Radiation Source at 2 GeV (*ca.* 3.2×10^{-10} J) with an average current of 190 mA in transmission mode, at room temperature, on stations 7:1 and 9:2 using an order sorting Si(111) or a double-crystal Si(220) monochromator offset to 50% of the rocking curve for harmonic rejection. Samples were diluted with dry boron nitride and mounted between Sellotape strips in 1 mm aluminium spacers. The EXAFS data treatment utilised the programs EX[8] and EXCURV 92.[9] Several data sets were collected for each compound in *k* space, and averaged to improve the signal-to-noise ratio. The pre-edge background was removed by fitting the spectrum to a quadratic polynomial, and subtracting this from the whole spectrum. The atomic contribution to the oscillatory part of the absorption spectrum was approximated using a polynomial, and the optimum function judged by minimising the intensity of chemically insignificant shells at low *r* in the Fourier transform. Curve fitting used single- or multiple-scattering curved-wave theory with phase shifts and backscattering factors calculated using normal *ab initio* methods.[10] Ground state potentials of the atoms were calculated using Von Barth theory and phase shifts using Hedin–Lundqvist potentials. The fits discussed below are for model data compared to raw (background-subtracted) EXAFS, and no Fourier filtering or smoothing has been applied. The distances and Debye–Waller factors were refined for all the shells, as well as the Fermi energy difference.

The ligands,[7] *cis*-[$PtCl_2(MeCN)_2$],[11] *cis*-[$PdCl_2(MeCN)_2$],[11] [{IrCl(COD)}$_2$][12] and [$\{PtCl_2(PEt_3)\}_2$][13] were prepared as previously described. The complexes, [$(RhCl_2Cp^*)_2$] and [$\{RhCl(CO)_2\}_2$] were commercial samples (Aldrich) and used as supplied. Dichloromethane, chloroform and perfluoro-1,3-dimethylcyclohexane (PP3) were each dried by refluxing over calcium hydride under dinitrogen, distilled under nitrogen and stored in closed ampoules over molecular sieves; PP3 was also frozen/pumped/thawed three times to remove all dissolved gases. Hexane was dried by refluxing over potassium metal under nitrogen, distilled and stored similarly. Toluene and diethyl ether were dried by refluxing over sodium metal under nitrogen, distilled and stored similarly.

Preparations

***trans*-[$PdCl_2\{PPh_2(C_6H_4C_6F_{13}-4)\}_2$] 11**. The ligand (0.348 g, 0.60 mmol) and *trans*-[$PdCl_2(MeCN)_2$] (0.078 g, 0.30 mmol) were stirred in refluxing dichloromethane (60 cm^3) under dinitrogen for 2 h. The solvent was removed *in vacuo*, the product washed with light petroleum (bp 40–60 °C), recrystallised from boiling light petroleum and dried *in vacuo* (yellow powder; yield 0.034 g, 65%). The corresponding *trans*-$[PdCl_2L_2]$ [$L = PPh(C_6H_4C_6H_{13}\text{-}4)_2$ or $P(C_6H_4C_6H_{13}\text{-}4)_3$] were made similarly. Yields 60–80%.

The corresponding *cis*-$[PtCl_2\{PPh_2(C_6H_4C_6F_{13}\text{-}4)\}_2]$ **14**, *cis*-$[PtCl_2\{PPh(C_6H_4C_6F_{13}\text{-}4)_2\}_2]$ **15** and a mixture of *cis*- and *trans*-$[PtCl_2\{P(C_6H_4C_6F_{13}\text{-}4)_3\}_2]$ **16** were made, as white powders, in the same way as their palladium analogues from $[PtCl_2(MeCN)_2]$. Yields 60–78%.

$[RhCl_2(\eta^5\text{-}C_5Me_5)\{PPh_2(C_6H_4C_6F_{13}\text{-}4)\}]$ 1. The ligand (0.144 g, 0.25 mmol) and $[(RhCl_2Cp^*)_2]$ (0.77 g, 0.12 mmol) were refluxed in ethanol (60 cm^3) under dinitrogen for 2 h. The solvent was removed *in vacuo* to yield a red solid which was recrystallised from CH_2Cl_2–hexane to give a fine red powder. Yield 0.15 g, 70%. The corresponding $[RhCl_2(\eta^5\text{-}C_5Me_5)L]$ were made similarly. Yields 75–81%.

***trans*-$[RhCl(CO)\{PPh_2(C_6H_4C_6F_{13}\text{-}4)\}_2]$ 4.** The ligand (0.270 g, 0.47 mmol) and $[\{RhCl(CO)_2\}_2]$ (0.044 g, 0.11 mmol) were stirred for 1.5 h under dinitrogen in CH_2Cl_2 (50 cm^3). The solvent was removed *in vacuo* to give a yellow powder which was washed with light petroleum (bp 40–60 °C) (2 × 10 cm^3). Yield 0.13 g, 66%. The corresponding *trans*-$[RhCl(CO)L_2]$ were made similarly. Yields 73–75%.

***trans*-$[IrCl(CO)\{PPh_2(C_6H_4C_6F_{13}\text{-}4)\}_2]$ 7.** The ligand (0.246 g, 0.42 mmol) and $[\{IrCl(COD)\}_2]$ (0.071 g, 0.11 mmol) were stirred in dry, degassed CH_2Cl_2 (15 cm^3) under a CO atmosphere (1 atm) for 30 min at room temperature. The solvent was removed *in vacuo*. Dry, degassed, hexane (5 cm^3) was added and the resulting yellow slurry stirred for 5 min to give a yellow solid which was quickly filtered in air and dried *in vacuo.* Yield 0.152 g, 70%. The corresponding *trans*-$[IrCl(CO)L_2]$ were made similarly. Yields 70–76%.

Mixture of *cis*- and *trans*-$[PtCl_2(PEt_3)\{P(C_6H_4C_6F_{13}\text{-}4)_3\}]$ 17. The ligand (0.68 g, 0.56 mmol) and $[\{PtCl_2(PEt_3)\}_2]$ (0.183 g, 0.28 mmol) were refluxed in dichloromethane (50 cm^3) for 3 h under nitrogen. After cooling to room temperature, the solvent was removed *in vacuo* to give a white solid which was washed with light petroleum (bp 40–60 °C), filtered and dried *in vacuo*. Yield 0.56 g, 63%.

Kinetic studies

Method 1. The *trans*-$[IrCl(CO)L_2]$ [$L = PPh_{3-x}(C_6H_4C_6F_{13}\text{-}4)_x$; $x = 0, 1, 2, 3$ or $L = P(C_6H_4CF_3\text{-}4)_3$] (12.8 μmol) was dissolved in chloroform (5 cm^3) which had been saturated with O_2 (8.52 μmol cm^{-3} at 20 °C)[14] in a closed system. The solution was stirred and O_2 was continually bubbled through the solution at room temperature. Samples (0.2 cm^3) were removed at regular intervals and the relative ratio of product:reactant measured by IR spectroscopy before the sample was returned to the reaction vessel.

Method 2. Three oxidation experiments were performed at 296 K with 20×, 15× and 10× molar excesses of oxygen respectively. The initial concentrations of O_2 were established by mixing appropriate aliquots of saturated (O_2 and N_2) solutions of chloroform. The same metal complexes (6.1 μmol) were dissolved in 14 cm^3 of each chloroform solution in a 10 cm^3 closed round-bottomed flask submersed in a thermostatically controlled water-bath. Product : reactant ratios were measured using the procedure outlined under method 1.

Solubility studies

The metal complexes (0.05 g), PP3 (1.5 cm^3) and [$^2H_8$]toluene (1.5 cm^3) were shaken in a test-tube and allowed to settle. The phases were separated by syringe, loaded into 4 or 5 mm outside diameter NMR tubes and $^{31}P\text{-}\{^1H\}$ NMR spectra recorded for each phase. A quantitative evaluation of the partition coefficients was not undertaken in view of the accuracy of integration associated with routine $^{31}P\text{-}\{^1H\}$ NMR experiments.[15]

Crystal structure determinations

$[RhCl_2(\eta^5\text{-}C_5Me_5)\{P(C_6H_4C_6F_{13}\text{-}4)_3\}]$ 3. *Crystal data.* $C_{46}H_{27}Cl_2F_{39}PRh$, $M = 1525.46$, monoclinic, $a = 7.911(3)$, $b = 45.183(13)$, $c = 15.330(2)$ Å, $\beta = 93.43(1)°$, $U = 5470(3)$ Å^3, $T = 150$ K, space group $P2_1/c$, $Z = 4$, $D_c = 1.852$ g cm^{-3}, $F(000) = 2992$, dimensions 0.18 × 0.14 × 0.10 mm, μ(Mo-Kα) = 0.608 mm^{-1}, 21472 reflections measured (Enraf Nonius FAST area detector diffractometer), 8258 unique ($R_{int} = 0.1835$) which were used in all calculations. The final $R1 = 0.079$, $wR(F^2)$ (all data) was 0.182.

***cis*- and *trans*-$[PtCl_2\{P(C_6H_4C_6F_{13}\text{-}4)_3\}_2]$ 16.** *Crystal data.* $C_{216}H_{72}Cl_6F_{234}P_6Pt_3$, $M = 4048.26$, triclinic, $a = 18.254(2)$, $b = 19.180(2)$, $c = 20.290(2)$ Å, $\alpha = 101.17(1)$, $\beta = 100.47(1)$, $\gamma = 92.76(1)°$, $U = 6827.5(12)$ Å^3, $T = 120$ K, space group $P\bar{1}$ (no. 2), $Z = 1$, $D_c = 1.969$ g cm^{-3}, $F(000) = 3900$, dimensions 0.66 × 0.33 × 0.31 mm, μ(Mo-Kα) = 1.838 mm^{-1}, 30707 reflections measured (Siemens P4 diffractometer), 27923 unique ($R_{int} = 0.0433$) which were used in all calculations. The final $R1 = 0.0816$, $wR(F^2)$ (all data) was 0.1818. The final Fourier-difference map had +1.7 and −1.2 e Å^{-3} peaks < 1 Å from the fluorine chain atoms [*i.e.* highest peak at 0.89 Å from F(112)].

CCDC reference number 186/1173.

See http://www.rsc.org/suppdata/dt/1998/3751/ for crystallographic files in .cif format.

Results and discussion

The reactions between the fluorous-derivatised triarylphosphine ligands and conventional platinum-group metal starting materials yield analogues of well established co-ordination and organometallic complexes either by the cleavage of chloride-bridged dimers or by the displacement of weakly co-ordinating ligands. The reactions are relatively straightforward affording, predominantly, air-stable metal products in reasonable (60–80%) yields which analyse well in view of the significant numbers of perfluoroalkyl ponytails. Spectroscopic studies on the platinum complexes of the tris-derivatised ligands (see below) indicated a mixture of *cis* and *trans* isomers which we were unable to separate even by recrystallisation. For the $[PtCl_2\{P(C_6H_4C_6F_{13}\text{-}4)_3\}_2]$ complex **16** we obtained single crystals suitable for X-ray crystallography and, remarkably, the *cis* and *trans* isomers co-crystallised (see below). For these complexes, the spectroscopic data reported below are, therefore, for these mixtures of isomers.

The complexes were characterised by FAB mass spectrometry, IR (Table 1), ^1H, ^{19}F and ^{31}P NMR spectroscopies (Table 2), EXAFS (Table 8) and single crystal X-ray diffraction. The mass spectra for most of the complexes showed either $[M - Cl]^+$ or $[M - CO]^+$ as the most intense fragments, in line with mass spectral data for many metal–phosphine complexes. Assignment of the co-ordination geometry for the $[MCl_2L_2]$ (M = Pd or Pt) comes from a combination of ^{31}P NMR data (see below) and ν(M–Cl). For M = Pd, a single IR active Pd–Cl stretch suggests a *trans* arrangement whilst for M = Pt [except when $L = P(C_6H_4C_6F_{13}\text{-}4)_3$] the observation of two Pt–Cl stretches implies a *cis* geometry. These results are in line with the thermodynamically favoured products in these systems established with conventional arylphosphine ligands.[17] For the platinum complexes with the tris-derivatised ligand, **16** and **17**, the observation of three Pt–Cl stretches offers the first evidence of the mixture of isomers for these complexes. The rhodium(I)

Table 1 Analytical, mass and IR spectral data

Complex	Analysis (%)[a] C	H	X[b]	m/z[c]	$\tilde{\nu}$(M–Cl) or $\tilde{\nu}$(CO)/cm^{-1}
1 $[RhCl_2(\eta^5\text{-}C_5Me_5)\{PPh_2(C_6H_4C_6F_{13}\text{-}4)\}]$	45.94(45.89)	3.30(3.26)	4.29(3.49)	853 $[(M-Cl)^+]$, 818 $[(M-2Cl)^+]$	–
2 $[RhCl_2(\eta^5\text{-}C_5Me_5)\{PPh(C_6H_4C_6F_{13}\text{-}4)_2\}]$	40.24(39.77)	2.19(2.32)	2.21(2.57)	1206 $[M^+]$, 1171 $[(M-Cl)^+]$, 1136 $[(M-2Cl)^+]$	–
3 $[RhCl_2(\eta^5\text{-}C_5Me_5)\{P(C_6H_4C_6F_{13}\text{-}4)_3\}]$	37.11(36.21)	1.94(1.79)	45.48(48.50)[d]	1524 $[M^+]$, 1489 $[(M-Cl)^+]$, 1454 $[(M-2Cl)^+]$	–
4 *trans*-$[RhCl(CO)\{PPh_2(C_6H_4C_6F_{13}\text{-}4)\}_2]$	44.32(44.33)	1.96(2.11)	21.47(37.24)[d]	1298 $[(M-CO)^+]$, 1263 $[(M-CO-Cl)^+]$	1982
5 *trans*-$[RhCl(CO)\{PPh(C_6H_4C_6F_{13}\text{-}4)_2\}_2]$	37.70(37.30)	1.16(1.32)	3.36(3.16)	1934 $[(M-CO)^+]$, 1899 $[(M-CO-Cl)^+]$	1983
6 *trans*-$[RhCl(CO)\{P(C_6H_4C_6F_{13}\text{-}4)_3\}_2]$	33.52(33.71)	0.92(0.92)	2.52(2.39)	2535 $[(M-CO-Cl)^+]$	1993
7 *trans*-$[IrCl(CO)\{PPh_2(C_6H_4C_6F_{13}\text{-}4)\}_2]$	40.58(40.62)	1.92(1.93)	4.82(4.28)	1416 $[(M+H)^+]$, 1381 $[(M+H-Cl)^+]$	1959 1972
8 *trans*-$[IrCl(CO)\{PPh(C_6H_4C_6F_{13}\text{-}4)_2\}_2]$	36.26(35.68)	0.91(1.27)	3.04(3.02)	1988 $[(M-CO-Cl)^+]$	
9 *trans*-$[IrCl(CO)\{P(C_6H_4C_6F_{13}\text{-}4)_3\}_2]$	32.39(32.60)	0.85(0.89)	3.81(2.31)	2688 $[M^+]$	1979
10 *trans*-$[IrCl(CO)\{P(C_6H_4CF_3\text{-}4)_3\}_2]$	43.37(43.45)	2.00(2.02)	4.99(5.22)	1188 $[M^+]$, 1160 $[(M-CO)^+]$	1975
11 *trans*-$[PdCl_2\{PPh_2(C_6H_4C_6F_{13}\text{-}4)\}_2]$	43.33(43.07)	1.97(2.09)	6.05(4.64)	1302$[(M+H-Cl)^+]$, 1266$[(M-2Cl)^+]$	364
12 *trans*-$[PdCl_2\{PPh(C_6H_4C_6F_{13}\text{-}4)_2\}_2]$	36.45(36.49)	1.30(1.32)	3.92(3.14)	1902$[(M-2Cl)^+]$	364
13 *trans*-$[PdCl_2\{P(C_6H_4C_6F_{13}\text{-}4)_3\}_2]$	33.33(33.11)	0.83(0.92)	2.03(2.38)	2538 $[(M-2Cl)^+]$	
14 *cis*-$[PtCl_2\{PPh_2(C_6H_4C_6F_{13}\text{-}4)\}_2]$	40.59(40.39)	1.71(1.96)	33.80(34.64)[d]	1391 $[(M+H-Cl)^+]$	364
15 *cis*-$[PtCl_2\{PPh(C_6H_4C_6F_{13}\text{-}4)_2\}_2]$	34.74(34.92)	1.06(1.26)	2.40(3.01)	2027 $[(M+H-Cl)^+]$, 1991 $[(M-2Cl)^+]$	323, 303 323, 303
16 *cis-/trans*-$[PtCl_2\{P(C_6H_4C_6F_{13}\text{-}4)_3\}_2]$	32.54(32.04)	0.93(0.90)	50.46(54.91)	2699 $[M^+]$, 2663$[(M-Cl)^+]$, 2627$[(M-2Cl)^+]$	340, 312, 292
17 *cis-/trans*-$[PtCl_2(PEt_3)\{P(C_6H_4C_6F_{13}\text{-}4)_3\}]$	31.71(31.51)	1.80(1.70)	45.25(46.29)[d]	1600 $[M^+]$, 1565 $[(M-Cl)^+]$	350, 316, 293

[a] Calculated values in parentheses. Microanalysis for metal complexes with perfluoroalkyl sidechains may be inaccurate due to poor combustion as described earlier.[16b] [b] X = P, unless otherwise stated. [c] Fast-atom bombardment with *m*-nitrobenzyl alcohol matrix. [d] X = F.

and iridium(I) complexes show a single band assignable as ν(CO). The variation in ν(CO) with electron density at the metal centre is well established and here, for each series, there is a general increase in ν(CO) (Table 3) with the addition of two fluorous ponytails (one per ligand). Interestingly, the effects of introducing a CF_3 group and a C_6F_{13} ponytail are similar. These results indicate that the phosphorus atoms and arene rings do not completely insulate the metal atoms from the highly electron withdrawing fluorous ponytails but, by comparison with the data for the closely related *trans*-$[IrCl(CO)\{P(C_2H_4C_6F_{13})_3\}_2]$ [ν(CO) 1977 cm^{-1}][16,20] and *trans*-$[IrCl(CO)(PEt_3)_2]$ [ν(CO) 1929 cm^{-1}],[21] the arene rings are better insulators than the linear ethyl spacers.

NMR Spectroscopic studies

For the Cp* rhodium complexes, the ^1H NMR spectra show, in addition to the aryl resonances associated with the ligands, doublets at *ca.* δ 1.2 readily assigned to the Cp* methyl protons. The hydrogen-phosphorus coupling constant (*ca.* 4 Hz) is typical for this class of complex. For the mixture of *cis*- and *trans*-$[PtCl_2(PEt_3)\{P(C_6H_4C_6F_{13}\text{-}4)_3\}]$ **17**, the observation of two well resolved sets of resonances for the ethyl groups confirms the presence of both isomers in solution. For the metal complexes containing ligands with one or two ponytails the aryl regions in the ^1H NMR spectra are complicated, overlapping, multiplets due to the C_6H_4 and C_6H_5 protons but, for the metal complexes with the $P(C_6H_4C_6F_{13}\text{-}4)_3$ ligand, the *ortho*- and *meta*-protons are resolved. In addition to the $^3J_{HH}$ interaction, the protons *ortho* to phosphorus show identifiable $^3J_{HP}$ couplings which can result in their ^1H NMR resonances appearing as triplets, as seen for the 'free' ligand.[7] The ^{19}F NMR spectra for all the complexes show five or six, highly consistent, multiplet resonances which are similar to those for the 'free' ligands. The highest frequency resonances are assigned to the terminal CF_3 groups. The remaining, CF_2, resonances are assigned according to Scheme 1 from ^{19}F–^{19}F COSY experiments.

$$\wr\!-C^{\alpha}F_2-C^{\beta}F_2-C^{\gamma}F_2-C^{\delta}F_2-C^{\varepsilon}F_2-CF_3$$

Scheme 1

The ^{31}P NMR spectral data offer further insights into the electronic influence of the perfluoroalkyl substituents. Except for complex **16** and **17**, the ^{31}P NMR spectra of these complexes exhibit a single resonance (M = Ir or Pd), a single resonance with satellites (M = Pt) or a doublet (M = Rh). For M = Pt (**14**, **15**), the $^1J_{PtP}$ coupling constants (3653 and 3635 Hz) confirm the *cis* configuration at the metal centre suggested from the IR data. For **16**, the observation of two singlets with significantly different coupling constants confirms the presence of both the *cis* and *trans* isomers in solution. Similarly for **17**, in addition to the resonances for the triethylphosphine ligand, the observation of two multiplets assignable to co-ordinated arylphosphines, a lower frequency multiplet with a large $^1J_{PtP}$ and a small $^2J_{PP}$ coupling constant consistent with a *cis*-$PtCl_2LL'$ arrangement and a higher frequency multiplet with a small $^1J_{PtP}$ and a large $^2J_{PP}$ coupling constant consistent with a *trans*-$PtCl_2LL'$ arrangement, confirm the presence of both isomers in solution. We have previously shown that $\delta(^{31}P)$ is insensitive to the electronic nature of the phosphorus atom whilst a variation in $^1J_{MP}$ is an indicator of electronic effects.[22] A comparison of the ^{31}P NMR spectral data with those for the analogous triphenylphosphine complexes (Table 4), particularly $\Delta^{31}P(\delta_{complex} - \delta_{free\ ligand})$ and $^1J_{MP}$, illustrates that there are general increases/decreases with the number of ponytails and that the introduction of perfluoroalkyl groups has a small influence on the electronic properties of the phosphine ligands. It has recently been argued[26] that for platinum(II) complexes a decrease in $^1J_{PtP}$ can be correlated with the Hammett constant (σ_P)[27] which can be rationalised in terms of decreased P$\rightarrow$Pt σ donation which occurs with electron-withdrawing substituents. Using their correlation, σ_P for $P(C_6H_4C_6F_{13}\text{-}4)_3$ can be estimated as 0.36, *cf.* 0.00 for PPh_3, which should result in a weaker Pt–P bond.[28]

Structural studies

During the course of this work we obtained crystals suitable for structural characterisation for two of the metal complexes.

Table 2 NMR Spectral data[a]

Complex	^1H	$^{19}F\text{-}\{^1H\}$	$^{31}P\text{-}\{^1H\}$
1	1.36 (15 H, d, J_{HP} 4, Cp*), 7.3–8.0 (14 H, m, C_6H_4/C_6H_5)	-81.2 (3F, t, $^3J_{FF}$ 10, CF_3), -111.5 (2F, t, $^3J_{FF}$ 14, $C^{\alpha}F_2$), -121.9 (2F, m, $C^{\beta}F_2$), -122.1 (2F, m, $C^{\delta}F_2$), -123.2 (2F, m, $C^{\varepsilon}F_2$), -126.5 (2F, m, $C^{\gamma}F_2$)	29.9 (d, $^1J_{RhP}$ 146)
2	1.37 (15 H, d, J_{HP} 4.5, Cp*), 7.3–8.0 (13 H, m, C_6H_4/C_6H_5)	-81.2 (3F, t, $^3J_{FF}$ 10, CF_3), -111.6 (2F, t, $^3J_{FF}$ 14, $C^{\alpha}F_2$), -121.8 (2F, m, $C^{\beta}F_2$), -122.0 (2F, m, $C^{\delta}F_2$), -123.2 (2F, m, $C^{\varepsilon}F_2$), -126.6 (2F, m, $C^{\gamma}F_2$)	30.2 (d, $^1J_{RhP}$ 144)
3[b]	1.19 (15 H, d, J_{HP} 4, Cp*), 7.64 (6 H, m, *m*-H of C_6H_4P), 7.97 (6 H, t, $^3J_{HP} = {}^3J_{HH} = 9$, *o*-H of C_6H_4P)	-81.6 (3F, t, $^3J_{FF}$ 10, CF_3), -111.8 (2F, t, $^3J_{FF}$ 14, $C^{\alpha}F_2$), -122.0 (2F, m, $C^{\beta}F_2$), -122.3 (2F, m, $C^{\delta}F_2$), -123.4 (2F, m, $C^{\varepsilon}F_2$), -126.8 (2F, m, $C^{\gamma}F_2$)	29.6 (d, $^1J_{RhP}$ 147)
4	7.2–7.8 (14 H, m, C_6H_4/C_6H_5)	-81.3 (3F, t, $^3J_{FF}$ 10, CF_3), -111.4 (2F, t, $^3J_{FF}$ 14, $C^{\alpha}F_2$), -121.8 (2F, m, $C^{\beta}F_2$), -122.1 (2F, m, $C^{\delta}F_2$), -123.2 (2F, m, $C^{\varepsilon}F_2$), -126.5 (2F, m, $C^{\gamma}F_2$)	28.8 (br)(r.t.) 30.0 (d, $^1J_{RhP}$ 127) (224 K)
5	7.3–7.9 (13 H, m, C_6H_4/C_6H_5)	-81.3 (3F, t, $^3J_{FF}$ 11, CF_3), -111.6 (2F, t, $^3J_{FF}$ 14, $C^{\alpha}F_2$), -121.9 (2F, m, $C^{\beta}F_2$), -122.1 (2F, m, $C^{\delta}F_2$), -123.2 (2F, m, $C^{\varepsilon}F_2$), -126.6 (2F, m, $C^{\gamma}F_2$)	29.9 (d, $^1J_{RhP}$ 129)
6	7.67 (6 H, d, $^3J_{HH}$ 9, *m*-H of C_6H_4P), 7.81 (6 H, t, $^3J_{HP} = {}^3J_{HH}$ 9, *o*-H of C_6H_4P)	-81.4 (3F, t, $^3J_{FF}$ 10, CF_3), -111.7 (2F, t, $^3J_{FF}$ 14, $C^{\alpha}F_2$), -121.9 (2F, m, $C^{\beta}F_2$), -122.1 (2F, m, $C^{\delta}F_2$), -123.2 (2F, m, $C^{\varepsilon}F_2$), -126.5 (2F, m, $C^{\gamma}F_2$)	30.0 (d, $^1J_{RhP}$ 131)
7	7.2–7.8 (14 H, m, C_6H_4/C_6H_5)	-81.2 (3F, t, $^3J_{FF}$ 10, CF_3), -111.5 (2F, t, $^3J_{FF}$ 14, $C^{\alpha}F_2$), -121.9 (2F, m, $C^{\beta}F_2$), -122.1 (2F, m, $C^{\delta}F_2$), -123.2 (2F, m, $C^{\varepsilon}F_2$), -126.5 (2F, m, $C^{\gamma}F_2$)	24.5 (s)
8	7.3–7.9 (13 H, m, C_6H_4/C_6H_5)	-81.2 (3F, t, $^3J_{FF}$ 10, CF_3), -111.6 (2F, t, $^3J_{FF}$ 14, $C^{\alpha}F_2$), -121.8 (2F, m, $C^{\beta}F_2$), -122.1 (2F, m, $C^{\delta}F_2$), -123.2 (2F, m, $C^{\varepsilon}F_2$), -126.6 (2F, m, $C^{\gamma}F_2$)	24.7 (s)
9	7.63 (6 H, d, $^3J_{HH}$ 8, *m*-H of C_6H_4P), 7.76 (6 H, dd, $^3J_{HP}$ 9.5, $^3J_{HH}$ 8, *o*-H of C_6H_4P)	-81.3 (3F, t, $^3J_{FF}$ 10, CF_3), -111.7 (2F, t, $^3J_{FF}$ 14, $C^{\alpha}F_2$), -121.9 (2F, m, $C^{\beta}F_2$), -122.1 (2F, m, $C^{\delta}F_2$), -123.3 (2F, m, $C^{\varepsilon}F_2$), -126.6 (2F, m, $C^{\gamma}F_2$)	24.7 (s)
10	7.70 (6 H, d, $^3J_{HH}$ 9, *m*-H of C_6H_4P), 7.84 (6 H, d, $^3J_{HH}$ 9, *o*-H of C_6H_4P)	-63.6 (s)	24.7 (s)
11	7.3–7.8 (14 H, m, C_6H_4/C_6H_5)	-81.3 (3F, t, $^3J_{FF}$ 10, CF_3), -111.5 (2F, t, $^3J_{FF}$ 12, $C^{\alpha}F_2$), -122.0 (4F, m, $C^{\beta}F_2/C^{\delta}F_2$), -123.2 (2F, m, $C^{\varepsilon}F_2$), -126.6 (2F, m, $C^{\gamma}F_2$)	23.6 (s)
12	7.4–7.9 (13 H, m, C_6H_4/C_6H_5)	-81.3 (3F, t, $^3J_{FF}$ 10, CF_3), -111.7 (2F, t, $^3J_{FF}$ 14, $C^{\alpha}F_2$), -122.0 (4F, m, $C^{\beta}F_2/C^{\delta}F_2$), -123.2 (2F, m, $C^{\varepsilon}F_2$), -126.6 (2F, m, $C^{\gamma}F_2$)	23.5 (s)
13	7.67 (6 H, d, $^3J_{HH}$ 8, *m*-H of C_6H_4P), 7.80 (6 H, dd, $^3J_{HP}$ 10, $^3J_{HH}$ 8, *o*-H of C_6H_4P)	-81.3 (3F, t, $^3J_{FF}$ 9, CF_3), -111.8 (2F, td, $^3J_{FF}$ 14, $^4J_{FF}$ 2, $C^{\alpha}F_2$), -122.0 (4F, t, $^3J_{FF}$ 9, $C^{\beta}F_2/C^{\delta}F_2$), -123.3 (2F, m, $C^{\varepsilon}F_2$), -126.6 (2F, m, $C^{\gamma}F_2$)	23.3 (s)
14	7.1–7.6 (14 H, m, C_6H_4/C_6H_5)	-81.2 (3F, t, $^3J_{FF}$ 12, CF_3), -111.6 (2F, t, $^3J_{FF}$ 14, $C^{\alpha}F_2$), -121.9 (2F, m, $C^{\beta}F_2$), -122.1 (2F, t, $^3J_{FF}$ 14, $C^{\delta}F_2$), -123.2 (2F, m, $C^{\varepsilon}F_2$), -126.5 (2F, m, $C^{\gamma}F_2$)	14.6 (s, $^1J_{PtP}$ 3635)
15	7.4–7.9 (13 H, m, C_6H_4/C_6H_5)	-81.3 (3F, t, $^3J_{FF}$ 9, CF_3), -111.8 (2F, t, $^3J_{FF}$ 14, $C^{\alpha}F_2$), -122.0 (4F, m, $C^{\beta}F_2/C^{\delta}F_2$), -123.3 (2F, m, $C^{\varepsilon}F_2$), -126.6 (2F, m, $C^{\gamma}F_2$)	14.6 (s, $^1J_{PtP}$ 3653)
16 (*cis*)[c]	7.82 (6 H, dd, $^3J_{HH}$ 8, $^3J_{HP}$ 11, *o*-H of C_6H_4P), 7.57 (6 H, d, $^3J_{HH}$ 8, *m*-H of C_6H_4P)	-82.2 (3F, t, $^3J_{FF}$ 10, CF_3), -112.1 (2F, t, $^3J_{FF}$ 13, $C^{\alpha}F_2$), -122.5 (4F, m, $C^{\beta}F_2/C^{\delta}F_2$), -123.8 (2F, m, $C^{\varepsilon}F_2$), -127.2 (2F, m, $C^{\gamma}F_2$)	15.5 (s, $^1J_{PtP}$ 3631)
16 (*trans*)[c]	7.95 (6 H, m, *o*-H of C_6H_4P), 7.79 (6 H, d, $^3J_{HH}$ 8, *m*-H of C_6H_4P)	-82.1 (3F, t, $^3J_{FF}$ 10, CF_3), -111.8 (2F, t, $^3J_{FF}$ 14, $C^{\alpha}F_2$), -122.5 (4F, m, $C^{\beta}F_2/C^{\delta}F_2$), -123.8 (2F, m, $C^{\varepsilon}F_2$), -127.2 (2F, m, $C^{\gamma}F_2$)	22.8 (s, $^1J_{PtP}$ 2719)
17 (*cis*)[c]	0.88 (9 H, dt, $^3J_{HP}$ 18, $^3J_{HH}$ 8, PCH_2CH_3), 1.56 (6 H, dq, $^2J_{HP}$ 10, $^3J_{HH}$ 8, PCH_2CH_3), 7.79 (6 H, d, $^3J_{HH}$ 8, *m*-H of C_6H_4P), 8.08 (6 H, dd, $^3J_{HP}$ 11, $^3J_{HH}$ 8, *o*-H of C_6H_4P)	-82.1 (3F, t, $^3J_{FF}$ 10, CF_3), -111.8 (2F, t, $^3J_{FF}$ 14, $C^{\alpha}F_2$), -122.3 (2F, m, $C^{\beta}F_2$), -122.6 (2F, m, $C^{\delta}F_2$), -123.8 (2F, m, $C^{\varepsilon}F_2$), -127.2 (2F, m, $C^{\gamma}F_2$)	10.1 (1P, d, $^1J_{PtP}$ 3285, $^2J_{PP}$ 15, PEt_3), 15.9 (1P, d, $^1J_{PtP}$ 3830, $^2J_{PP}$ 15, aryl P)
17 (*trans*)[c]	1.11 (9 H, m, PCH_2CH_3), 1.91 (6 H, m, PCH_2CH_3), 7.74 (6 H, d, $^3J_{HH}$ 8, *m*-H of C_6H_4P), 7.9 (6 H, vt, $^3J_{HH}$ 8, $^3J_{HP}$ 10, *o*-H of C_6H_4P)	-82.1 (3F, t, $^3J_{FF}$ 10, CF_3), -111.7 (2F, t, $^3J_{FF}$ 15, $C^{\alpha}F_2$), -122.3 (2F, m, $C^{\beta}F_2$), -122.6 (2F, m, $C^{\delta}F_2$), -123.8 (2F, m, $C^{\varepsilon}F_2$), -127.2 (2F, m, $C^{\gamma}F_2$)	18.1 (1P, d, $^1J_{PtP}$ 2640, $^2J_{PP}$ 472, PEt_3), 24.2 (1P, d, $^1J_{PtP}$ 2401, $^2J_{PP}$ 427, aryl P)

[a] Spectra recorded at room temperature in $CDCl_3$ unless otherwise stated. Data given as δ (intensity, multiplicity, J/Hz, assignment). [b] In CD_2Cl_2. [c] In $(CD_3)_2CO$.

Table 3 Variation of $\tilde{\nu}$(CO)[a] in *trans*-[MCl(CO)L_2] (M = Rh or Ir) with the number of perfluoroalkyl groups

Ligand	Rh	Ir
PPh_3	1965[b]	1953[c]
$PPh_2(C_6H_4C_6F_{13}\text{-}4)$	1982	1959
$PPh(C_6H_4C_6F_{13}\text{-}4)_2$	1983	1972
$P(C_6H_4C_6F_{13}\text{-}4)_3$	1993	1979
$P(C_6H_4CF_3\text{-}4)_3$	1990[b]	1975

[a] $\tilde{\nu}$(CO)/cm^{-1}. Recorded as Nujol mulls, unless otherwise stated. [b] In CH_2Cl_2 solution. Data taken from ref. 18. [c] Data taken from ref. 19.

These represent only the third and fourth structural characterisations of metal complexes with fluorous ponytails[16,20,29] and, in spite of the interest in the structural characteristics of perfluoro-aliphatic derivatives,[30,31] relatively few compounds with five or six CF_2 units have been crystallographically characterised.[32,33] Here, metal complexes with three and nine independent fluorous ponytails have been determined.

In [$RhCl_2(\eta^5\text{-}C_5Me_5)\{P(C_6H_4C_6F_{13}\text{-}4)_3\}$] **3** (Figs. 1 and 2; Table 5) the asymmetric unit cell contains one discrete molecule which adopts an archetypal piano-stool geometry. Considering the C_5Me_5 ring as a single co-ordination centre represented by its centroid, the rhodium co-ordination might be described as very distorted tetrahedral in which the bulky Cp* ligand forces

Table 4 $^{31}P-\{^1H\}$ NMR data for related arylphosphine metal complexes[a]

	$[RhCl_2(\eta^5-C_5Me_5)L]$		*trans*-$[RhCl(CO)L_2]$		*trans*-$[IrCl(CO)L_2]$	*trans*-$[PdCl_2L_2]$	*cis*-$[PtCl_2L_2]$	
Ligand	$\Delta(^{31}P)$	$^1J_{MP}$	$\Delta(^{31}P)$[a]	$^1J_{MP}$	$\Delta(^{31}P)$	$\Delta(^{31}P)$	$\Delta(^{31}P)$	$^1J_{MP}$
PPh_3	35.2	144	29.5[b]	125	28.5[c]	33.5[d]	18.9[e]	3676[e]
$PPh_2(C_6H_4C_6F_{13}-4)$	34.9	146	35.0[b]	127	29.5	28.0	19.6	3653
$PPh(C_6H_4C_6F_{13}-4)_2$	35.6	144	35.4	129	30.2	28.9	20.0	3635
$P(C_6H_4C_6F_{13}-4)_3$	35.6	147	36.0	131	30.7	29.3	21.5	3631
$P(C_6H_4CF_3-4)_3$	—	—	36.8	121	30.1	—	19.9[f]	3648[f]

[a] $\Delta(^{31}P) = \delta_{\text{metal complex}} - \delta_{\text{free ligand}}$/ppm, $^1J_{MP}$/Hz. [b] Spectrum recorded at 224 K. [c] Data taken from ref. 23. [d] Data taken from ref. 24. [e] Data taken from ref. 25. [f] Data taken from ref. 26.

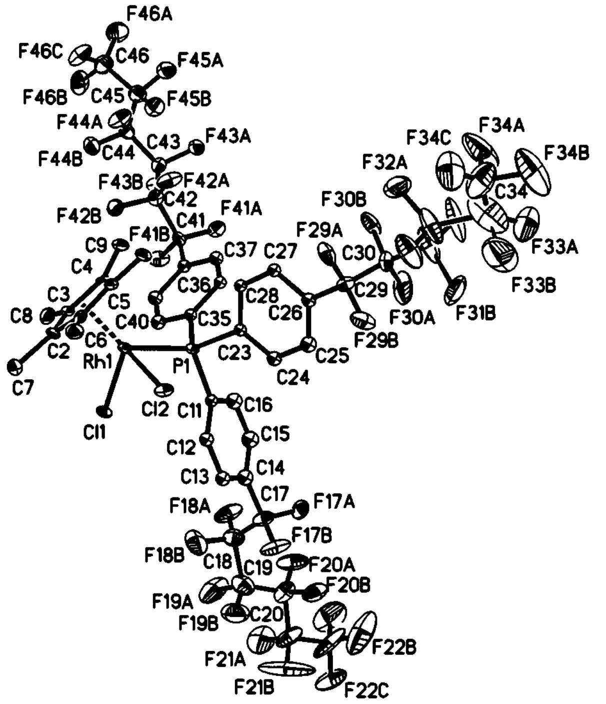

Fig. 1 Molecular structure of $[RhCl_2(\eta^5-C_5Me_5)\{P(C_6H_4C_6F_{13}-4)_3\}]$. Displacement ellipsoids are shown at the 30% probability level. The H atoms are omitted for clarity.

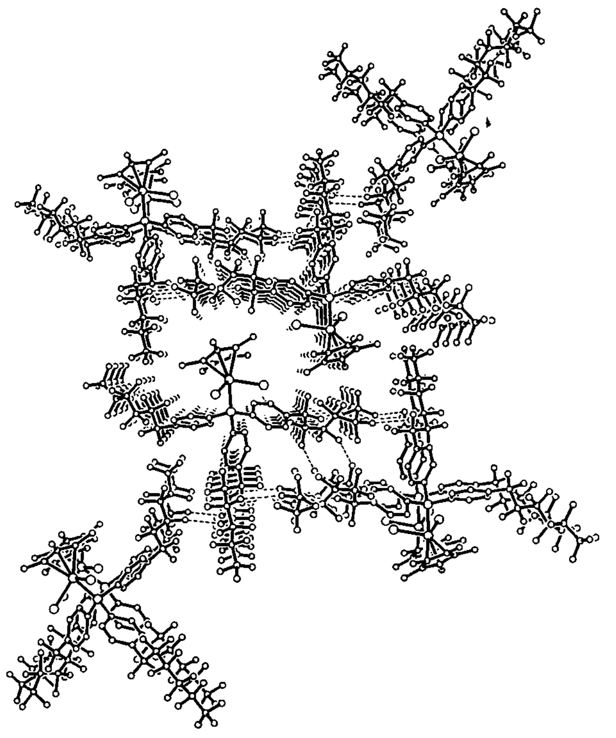

Fig. 2 Extended structure of $[RhCl_2(\eta^5-C_5Me_5)\{P(C_6H_4C_6F_{13}-4)_3\}]$ showing short intramolecular interactions.

the interligand angles between the other ligands close to 90°. Surprisingly, there have been relatively few structural characterisations on $[RhCl_2Cp^*L]$ [where L = phosphorus(III) donor ligand] complexes.[22,34–36] For **3**, the Rh–C_{Cp^*} and Rh–Cl distances are within the range defined by this group of complexes, and the Rh–P distance at 2.332(3) Å is close to the longest [2.327(5) Å, L = $PPh_2(C_2H_4SiMe_2OH)$], but this is not particularly surprising since the other crystallographically characterised complexes include trialkyl phosphite and triarylphosphonite ligands. Similarly, the slight asymmetry in the P–Rh–Cl and Cl–Rh–Cl bond angles is mirrored by this group of complexes and it can be concluded that, for this complex, the perfluoroalkyl groups have a negligible influence on the metal co-ordination environment in line with the NMR data. The perfluoroalkyl groups radiate away from the metal centre and, although the terminal CF_2CF_3 units have large thermal ellipsoids as a result of motion even at 150 K, in marked contrast to the previously characterised iridium and rhodium complexes with the $P(C_2H_4C_6F_{13})_3$ ligand,[16,20,29] this complex does not suffer from any disorder. The perfluoroalkyl groups experience the usual steric congestion resulting in twisting of the CF_2 units with respect to each other. There are two types of C_6F_{13} ponytails. The first, extending from C38, adopts a consistently *trans* and staggered conformation with torsion angles between 162 and 166° resulting in a linear ponytail. Here, the C–C bond lengths are similar and unremarkable. The others include a pseudo boat, *cis* conformation in the middle of the perfluoroalkyl chain where the torsion angle is much smaller (38 or 54°) causing the ponytail to kink. In these chains there is an alternation of long and short C–C distances which appear to be associated with the strained conformation. In an extended view of the lattice (Fig. 2), the preference for the perfluoroalkyl chains to align is illustrated and it is this interaction which appears to be important in holding the structure together. This strong preference has been highlighted previously[16,20,29] and appears to arise from electrostatic interactions between fluorous fragments which underpin the fluorous biphase concept. Here, there are a number of short F · · · F contacts between adjacent molecules. Most of the interactions involve the chains radiating from C29 holding pairs of molecules together and these chains point towards chains radiating from C17 and both sets of chains appear to have to kink to accommodate this arrangement.

As indicated by the spectroscopic data, $[PtCl_2\{P(C_6H_4C_6F_{13}-4)_3\}_2]$ **16** exists in the solid state and in solution as a mixture of *cis* and *trans* isomers. Single crystals of this complex were grown by slow evaporation of an acetone solution over 4 weeks. The very large unit cell contains 465 non-hydrogen atoms and the thermal motion of the perfluoroalkyl groups necessitated collecting the data at 120 K. The structure is highly unusual since it possesses both the *cis* and the *trans* isomers of the complex in the same unit cell in a 2 : 1 ratio. The asymmetric unit has one *cis*-molecule in a general position of the space group $P\bar{1}$ and half of a *trans*-molecule with the platinum atom located at

Table 5 Selected bond lengths (Å), angles (°), torsion angles (°) and non-bonded short interchain distances (Å) with estimated standard deviations (e.s.d.s) in parentheses for [RhCl$_2$(η^5-C$_5$Me$_5$){P(C$_6$H$_4$C$_6$F$_{13}$-4)$_3$}][a] **3**

Rh(1)–C(1)	2.215(9)	Rh(1)–C(2)	2.204(9)
Rh(1)–C(3)	2.164(9)	Rh(1)–C(4)	2.201(8)
Rh(1)–C(5)	2.179(9)	Rh(1)–Cl(1)	2.393(2)
Rh(1)–Cl(2)	2.398(3)	Rh(1)–P(1)	2.332(3)
Cp† ··· Rh(1)	1.824	av. P–C	1.831
av. C(cp*)–C(cp*)	1.431	av. C(cp*)–C(Me)	1.498
av. C(ring)–C(ring)	1.38	av. C(ring)–C(tail)	1.517
C(17)–C(18)	1.47(2)	C(18)–C(19)	1.63(2)
C(19)–C(20)	1.46(2)	C(20)–C(21)	1.65(2)
C(21)–C(22)	1.45(3)	C(29)–C(30)	1.499(14)
C(30)–C(31)	1.56(2)	C(31)–C(32)	1.30(2)
C(32)–C(33)	1.75(3)	C(33)–C(34)	1.16(3)
C(41)–C(42)	1.544(14)	C(42)–C(43)	1.547(14)
C(43)–C(44)	1.52(2)	C(44)–C(45)	1.57(2)
C(45)–C(46)	1.51(2)	av. C–F	1.375
P(1)–Rh(1)–Cl(1)	88.28(9)	P(1)–Rh(1)–Cl(2)	86.00(9)
Cl(1)–Rh(1)–Cl(2)	93.95(9)	C(11)–P(1)–Rh(1)	118.2(2)
C(23)–P(1)–Rh(1)	113.0(2)	C(35)–P(1)–Rh(1)	113.0(2)
C(11)–P(1)–C(23)	102.3(3)	C(11)–P(1)–C(35)	102.5(3)
C(23)–P(1)–C(35)	106.4(3)	P(1)–Rh(1) ··· Cp†	134.7
Cl(1)–Rh(1) ··· Cp†	120.5	Cl(2)–Rh(1) ··· Cp†	122.0
C(14)–C(17)–C(18)–C(19)	−167.8	C(17)–C(18)–C(19)–C(20)	−53.8
C(18)–C(19)–C(20)–C(21)	−171.4	C(19)–C(20)–C(21)–C(22)	178.9
C(26)–C(29)–C(30)–C(31)	−176.1	C(29)–C(30)–C(31)–C(32)	−37.8
C(30)–C(31)–C(32)–C(33)	176.1	C(31)–C(32)–C(33)–C(34)	151.8
C(38)–C(41)–C(42)–C(43)	165.9	C(41)–C(42)–C(43)–C(44)	162.6
C(42)–C(43)–C(44)–C(45)	163.3	C(43)–C(44)–C(45)–C(46)	165.5
F(17A) ··· F(34B)	2.791	F(19B) ··· F(33B)	2.662
F(20A) ··· F(43B)	2.697	F(29B) ··· F(34A)	2.815
F(30A) ··· F(31B)	2.789	F(31A) ··· F(31A)	2.701
F(31A) ··· F(33A)	2.880		

[a] Cp† denotes the cyclopentadienyl centroid.

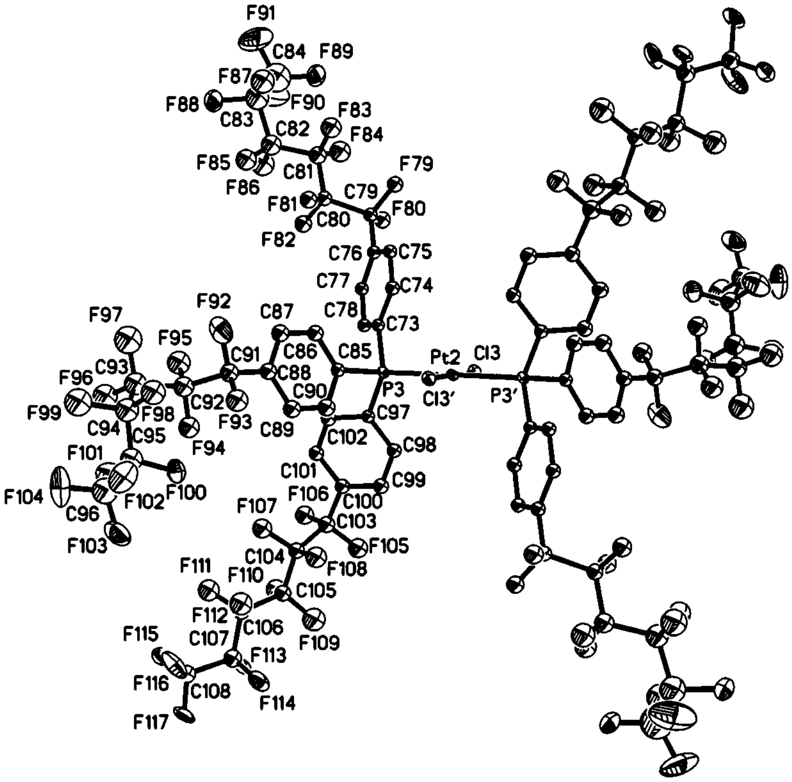

Fig. 3 Molecular structure of *trans*-[PtCl$_2${P(C$_6$H$_4$C$_6$F$_{13}$-4)$_3$}$_2$]. Details as in Fig. 1. Primed atoms generated by symmetry ($-x$, $-y$, $1 - z$).

the special position (0, 0, ½). Selected bond lengths and bond angles are given in Table 6 and the molecular structures of the two isomers are shown in Figs. 3 and 4. For the *trans* isomer the *trans* geometry and planarity of the "PtCl$_2$P$_2$" unit is imposed by crystallographic constraints. For the *cis* isomer the geometry around the metal atom is very similar to that for *cis*-[PtCl$_2$(PPh$_3$)$_2$],[37] *i.e.* there is slight asymmetry in the Pt–P and Pt–Cl bond lengths and the bond distances and angles at

Table 6 Selected bond lengths (Å), angles (°) and torsion angles (°) with estimated standard deviations (e.s.d.s) in parentheses for the mixture of *cis*- and *trans*-[PtCl$_2${P(C$_6$H$_4$C$_6$F$_{13}$-4)$_3$}$_2$] **16**

cis			
Pt(1)–Cl(1)	2.349(3)	Pt(1)–Cl(2)	2.328(2)
Pt(1)–P(1)	2.254(3)	Pt(1)–P(2)	2.271(3)
C(7)–C(8)	1.55(2)	C(8)–C(9)	1.58(2)
C(9)–C(10)	1.56(2)	C(10)–C(11)	1.46(2)
C(11)–C(12)	1.61(2)	C(19)–C(20)	1.47(2)
C(20)–C(21)	1.71(2)	C(21)–C(22)	1.40(2)
C(22)–C(23)	1.64(2)	C(23)–C(24)	1.45(2)
C(31)–C(32)	1.57(2)	C(32)–C(33)	1.56(2)
C(33)–C(34)	1.57(2)	C(34)–C(35)	1.55(2)
C(35)–C(36)	1.57(2)	C(43)–C(44)	1.58(2)
C(44)–C(45)	1.54(2)	C(45)–C(46)	1.56(2)
C(46)–C(47)	1.57(2)	C(47)–C(48)	1.56(2)
C(55)–C(56)	1.57(2)	C(56)–C(57)	1.56(2)
C(57)–C(58)	1.54(2)	C(58)–C(59)	1.58(2)
C(59)–C(60)	1.55(2)	C(67)–C(68)	1.54(2)
C(68)–C(69)	1.55(2)	C(69)–C(70)	1.52(2)
C(70)–C(71)	1.53(2)	C(71)–C(72)	1.43(2)
C(71)–C(72′)	1.43(2)	C(79)–C(80)	1.59(2)
P(1)–Pt(1)–P(2)	97.73(9)	P(1)–Pt(1)–Cl(2)	174.28(9)
P(1)–Pt(1)–Cl(1)	89.97(9)	P(2)–Pt(1)–Cl(1)	171.01(9)
P(2)–Pt(1)–Cl(2)	86.36(9)	Cl(2)–Pt(1)–Cl(1)	86.30(9)
C(1)–P(1)–Pt(1)	115.7(3)	C(13)–P(1)–Pt(1)	113.7(3)
C(25)–P(1)–Pt(1)	112.7(3)	C(37)–P(2)–Pt(1)	110.1(3)
C(49)–P(2)–Pt(1)	114.8(3)	C(61)–P(2)–Pt(1)	119.5(3)
C(1)–P(1)–C(13)	100.1(5)	C(1)–P(1)–C(25)	103.8(4)
C(13)–P(1)–C(25)	109.7(5)	C(37)–P(2)–C(49)	104.5(4)
C(37)–P(2)–C(61)	103.7(4)	C(49)–P(2)–C(61)	102.6(4)
C(4)–C(7)–C(8)–C(9)	−171.68	C(7)–C(8)–C(9)–C(10)	−168.01
C(8)–C(9)–C(10)–C(11)	−51.99	C(9)–C(10)–C(11)–C(12)	−162.73
C(16)–C(19)–C(20)–C(21)	−169.84	C(19)–C(20)–C(21)–C(22)	−50.06
C(20)–C(21)–C(22)–C(23)	−168.81	C(21)–C(22)–C(23)–C(24)	−165.00
C(28)–C(31)–C(32)–C(33)	174.25	C(31)–C(32)–C(33)–C(34)	169.55
C(32)–C(33)–C(34)–C(35)	167.21	C(33)–C(34)–C(35)–C(36)	164.06
C(40)–C(43)–C(44)–C(45)	175.81	C(43)–C(44)–C(45)–C(46)	−179.81
C(44)–C(45)–C(46)–C(47)	−179.77	C(45)–C(46)–C(47)–C(48)	175.28
C(52)–C(55)–C(56)–C(57)	165.27	C(55)–C(56)–C(57)–C(58)	159.43
C(56)–C(57)–C(58)–C(59)	162.30	C(57)–C(58)–C(59)–C(60)	163.85
C(64)–C(67)–C(68)–C(69)	−171.72	C(67)–C(68)–C(69)–C(70)	−168.02
C(68)–C(69)–C(70)–C(71)	−167.30	C(69)–C(70)–C(71)–C(72)	−48.57
trans			
Pt(2)–Cl(3)	2.331(2)	Pt(2)–P(3)	2.330(3)
C(80)–C(81)	1.54(2)	C(81)–C(82)	1.58(2)
C(82)–C(83)	1.62(2)	C(83)–C(84)	1.40(2)
C(91)–C(92)	1.57(2)	C(92)–C(93)	1.63(2)
C(93)–C(94)	1.45(2)	C(94)–C(95)	1.43(2)
C(95)–C(96)	1.67(2)	C(103)–C(104)	1.58(2)
C(104)–C(105)	1.55(2)	C(105)–C(106)	1.58(2)
C(106)–C(107)	1.53(2)	C(107)–C(108)	1.54(2)
P(3)–Pt(2)–Cl(3)	86.66(9)	P(3)–Pt(2)–P(3′)	180.0
P(3)–Pt(2)–Cl(3′)	93.34	Cl(3)–Pt(2)–Cl(3′)	180.0
C(73)–P(3)–Pt(2)	108.9(3)	C(85)–P(3)–Pt(2)	116.2(3)
C(97)–P(3)–Pt(2)	115.3(3)	C(73)–P(3)–C(85)	105.8(5)
C(85)–P(3)–C(97)	101.5(5)	C(73)–P(3)–C(97)	108.7(5)
C(76)–C(79)–C(80)–C(81)	166.96	C(79)–C(80)–C(81)–C(82)	168.37
C(80)–C(81)–C(82)–C(83)	160.98	C(81)–C(82)–C(83)–C(84)	63.97
C(88)–C(91)–C(92)–C(93)	−172.04	C(91)–C(92)–C(93)–C(94)	−60.57
C(92)–C(93)–C(94)–C(95)	−57.18	C(93)–C(94)–C(95)–C(96)	−160.52
C(100)–C(103)–C(104)–C(105)	−171.68	C(103)–C(104)–C(105)–C(106)	−171.68
C(104)–C(105)–C(106)–C(107)	−163.73	C(105)–C(106)–C(107)–C(108)	−163.66
Non-bonded short interchain distances (Å) for the mixture			
F(7)···F(96)	2.833	F(21)···F(21)	2.875
F(13)···F(69)	2.802	F(16)···F(91)	2.831
F(27)···F(33)	2.745	F(32)···F(76′)	2.720
F(41)···F(78)	2.819	F(41)···F(78′)	2.828
F(43)···F(65)	2.845	F(53)···F(82)	2.696
F(63)···F(95)	2.782	F(71)···F(99)	2.783
F(76′)···F(108)	2.597	F(89)···F(101)	2.852
F(99)···F(104)	2.603	F(101)···F(104)	2.736
F(101)···F(102)	2.836	F(102)···F(104)	2.147
F(103)···F(104)	2.098	F(110)···F(115)	2.754

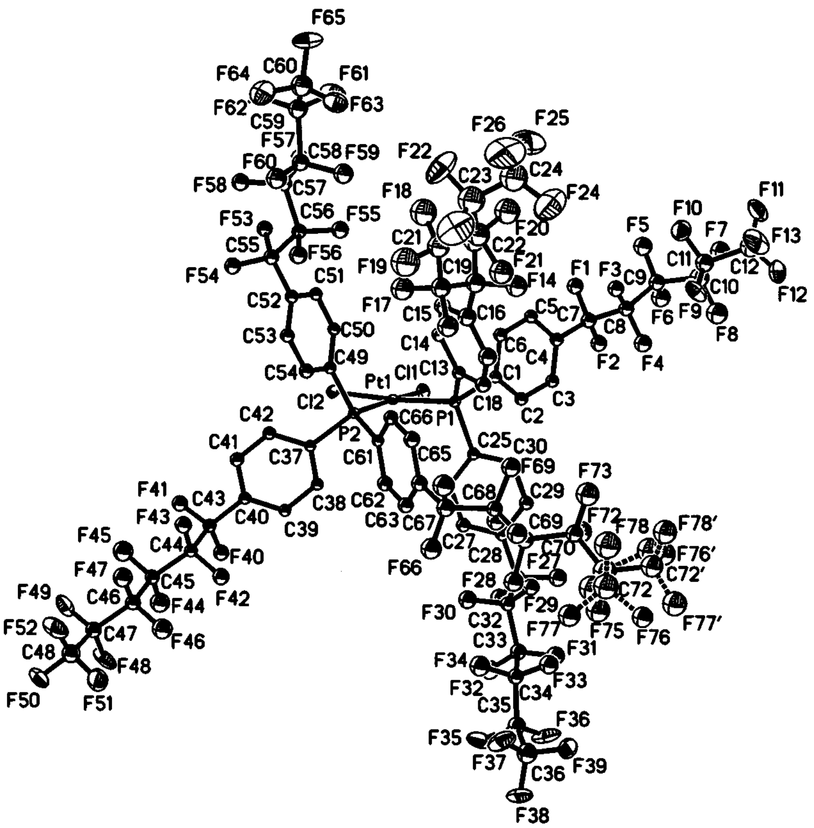

Fig. 4 Molecular structure of *cis*-[PtCl$_2${P(C$_6$H$_4$C$_6$F$_{13}$-4)$_3$}$_2$]. Details as in Fig. 1. Disorder indicated by dashed bonds.

platinum for both *cis* complexes in the essentially planar "PtCl$_2$P$_2$" cores are virtually identical. In particular, the insignificant differences between the platinum–phosphorus bond lengths for **16** [2.254(3) and 2.271(3) Å] and those for *cis*-[PtCl$_2$(PPh$_3$)$_2$] [2.251(2) and 2.265(2) Å] suggest the introduction of the electron withdrawing perfluoroalkyl chains appears to have little influence on the length of the Pt–P bond. Phosphorus(1) is slightly closer to platinum than phosphorus(2) and, consequently, has a larger influence on the angles at the metal centre. The Pt–P bond lengths in the *cis* isomer are shorter than that for the *trans* isomer, in line with the difference in the *trans* influence between chloride and phosphorus. The P–C, C–C and C–F bond lengths in the nine unique substituents on the phosphorus atoms are very similar and are entirely consistent with co-ordinated phosphines[38] and highly fluorinated aliphatic compounds.[16,20,29–31] It has been suggested that the variation in Pt–P–C angles reflects the degree of overcrowding at the metal centre for these square planar [PtCl$_2$(phosphine)$_2$] complexes. Here, only phosphorus(2) shows any significant asymmetry in the Pt–P–C angles (which is translated into a longer Pt–P distance), and the largest Pt–P–C angle is 3° smaller than that for *cis*-[PtCl$_2$(PPh$_3$)$_2$][37] implying that the fluorous-ponytail-derivatised ligand has *less* steric bulk than its protio-congener. The perfluoroalkyl groups radiate away from the metal centres and one chain, that radiating from C64, experiences disorder of the CF$_3$ group and a fluorine atom on C71, the two arrangements occurring in a 50 : 50 ratio. This disorder is similar to that observed for *trans*-[MCl(CO){P(C$_2$H$_4$-C$_6$F$_{13}$)$_3$}$_2$] (M = Rh or Ir).[16,20,29] The nine unique fluorous ponytails adopt three different conformations (Fig. 5). Four (radiating from C28, C40, C52 and C100) adopt the *trans* and staggered conformation (torsion angles vary from 159 to 180°) giving virtually linear perfluoroalkyl chains. Four (radiating from C4, C16, C64 and C76) contain one *cis* conformation (torsion angles of 52, 50, 49 and 64° respectively), although the location of this varies along the ponytail, affording kinked ponytails. These structural motifs are the same as those seen for [RhCl$_2$(η^5-C$_5$Me$_5$){P(C$_6$H$_4$C$_6$F$_{13}$-4)$_3$}] and a similar, although not as varied, distribution of C–C bond lengths is also present. The ponytail radiating from C88 is unique. Here, two adjacent *cis* conformations (torsion angles of 61 and 57°) result in a perfluoroalkyl unit which bends at virtually 90° in the middle. The extended view of this structure is not as straightforward as that for **3**. The perfluoroalkyl chains still lie in layers within the structure but are criss-crossed. Short interchain interactions, similar to those seen for **3**, hold the extended structure together. These interactions are predominantly associated with the bent perfluoroalkyl chains, however there are also interactions with the near-linear chains. The unique double-bent chain (radiating from C88) is interesting since it points directly at an identical chain eminating from an adjacent molecule (Fig. 6). The double bending is, therefore, necessary to accommodate these two chains. Even with this arrangement this area is very crowded with five short intermolecular interactions between the terminal C$_3$F$_7$ units including two extremely short distances (2.098 and 2.147 Å) between fluorines on the terminal CF$_3$ groups. However, these short interactions do not appear to influence the C–C bond lengths which are as regular as those for the straight ponytails.

One of the important aims of this work was to evaluate the effect of the perfluoroalkyl substituents on the donor properties of these ligands and, consequently, on the properties of their co-ordination compounds. As indicated above, the spectroscopic probes do not offer a clear-cut view of these effects. We have been unable to obtain single crystals suitable for structural determination for all of the co-ordination compounds described in this work, however an assessment of the structural impact of the ponytails can be made from variations in the metal's first co-ordination sphere. We have shown that the EXAFS technique can be a valuable probe of the metal co-ordination sphere which does not require single crystals.[39] Hence, we have collected and modelled the metal-edge EXAFS data for **4**–**9**, **11**–**15**, together with structurally characterised analogues as models to test the reliability of our data collection and treatment (Tables 7 and 8). For each complex, transmission EXAFS data were collected to $k = 15$ Å^{-1} (k = photoelectron

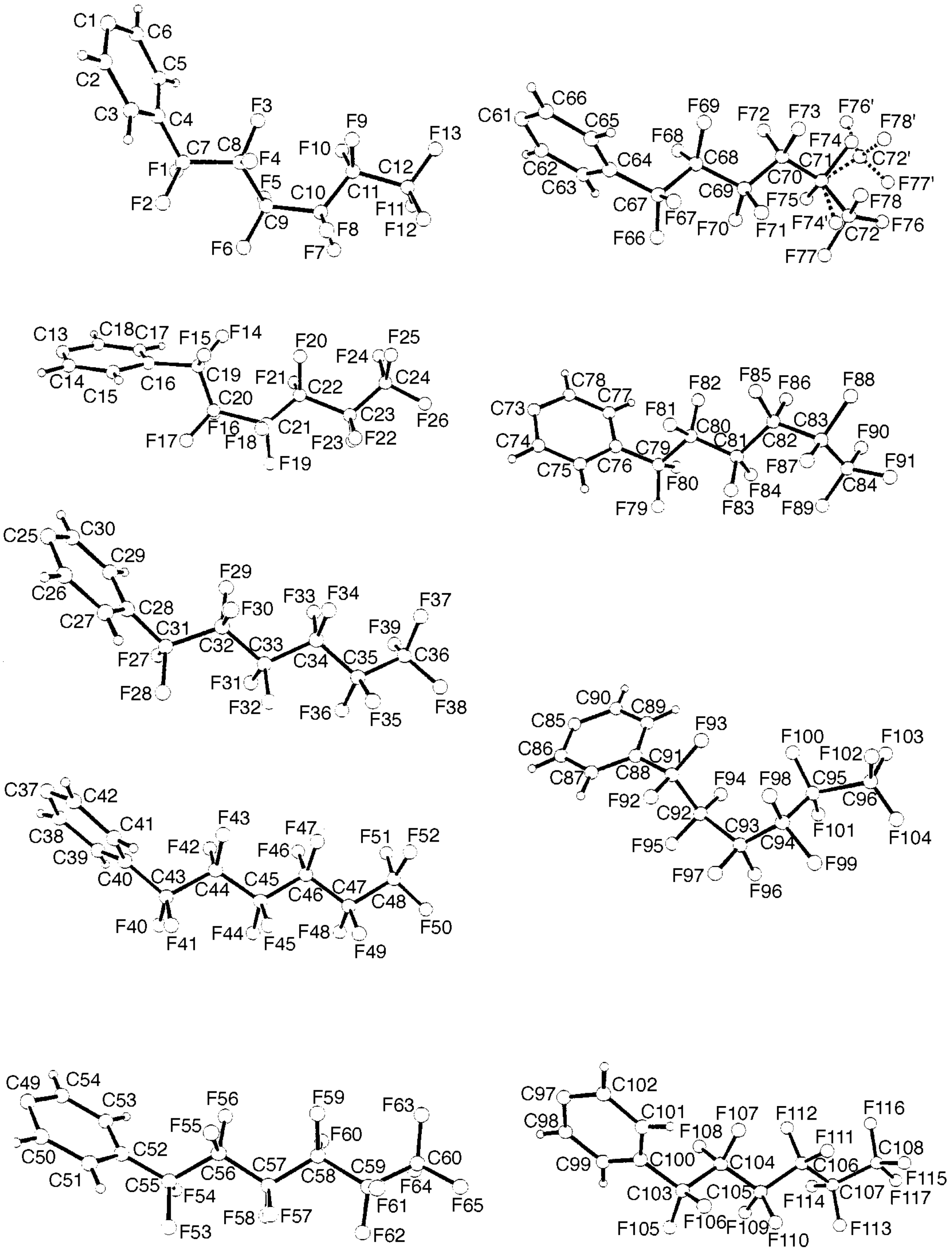

Fig. 5 Nine unique perfluoroalkyl groups present in $[PtCl_2\{P(C_6H_4C_6F_{13}\text{-}4)_3\}_2]$.

wave vector) beyond the edge but, due to poor signal-to-noise ratio at high k, the data were, typically, truncated at $k = 12.5$ Å^{-1}. At least five data sets were collected for each complex, averaged and the data multiplied by k^3 to compensate for drop-off in intensity at higher k. No smoothing or Fourier filtering was applied and the fits discussed below are compared with the averaged raw (background-subtracted) EXAFS data. Throughout the analyses we have iterated the distances and Debye–Waller factors for each shell and the Fermi energy; each shell was added stepwise and the best fits tested for statistical significance in the usual way.[42,43]

For the $[MCl_2L_2]$ (M = Pd or Pt) complexes the data were modelled to a two-shell model (2Cl, 2P). Although the Fourier transforms revealed features associated with longer non-bonding interactions and even though modelling these distances to carbon atoms in the backbone of the ligands resulted in significant reductions in the Fit Index and R factors, since we are interested in only the metal co-ordination environment we follow convention[44] in not modelling these longer interactions. We note that fitting two shells at similar distance may be dangerous. However, the validity of the fits we obtained can be demonstrated by the level of correlation between the two shells (<0.7) and our attempts to fit the data to chemically unreasonable single- or two-shell (3Cl, 1P and 1Cl, 3P) models which gave uncharacteristic Debye–Waller factors, unreasonable bond lengths and markedly poorer fits. The very good agreement between the EXAFS and crystallographic data for the triphenylphosphine complexes (Table 7) illustrates the reliability and value of the application of EXAFS to this system. Furthermore, these data for the model complexes compare very well with those for the perfluoroalkyl-derivatised metal complexes (Tables 6 and 8) indicating that, within the accuracy of the

EXAFS analysis, the co-ordination environment at the metal centre for **11**–**16** is not significantly affected by the introduction of the perfluoroalkyl substituents.

A similar analysis procedure for the *trans*-[MCl(CO)L$_2$] (M = Rh or Ir) used a three-shell model (1C, 3P, 1O) with multiple scattering for the non-bonded oxygen shell with a fixed M–C–O angle of 180° (Fig. 7). For this set of complexes we found that in a four-shell model (1C, 2P, 1Cl, 1O) the phosphorus and chlorine shells were very strongly correlated which significantly reduced the confidence in the modelling. Hence, we adopted the three-shell model in which the heavier backscatterers were modelled using a single shell of three phosphorus atoms. For the model compounds (Table 7) this gave entirely reasonable, averaged, distances and, again, the close agreement between the data for these model compounds and the perfluoroalkyl-derivatised species indicates that the perfluoroalkyl substituents have, within the accuracy of the EXAFS analysis, little influence on the metal co-ordination environment. These results indicate that the aryl spacer group is a good insulator of the electronic influence of the perfluoroalkyl ponytail and that any effects which are still present can be balanced by other factors at the metal centres.

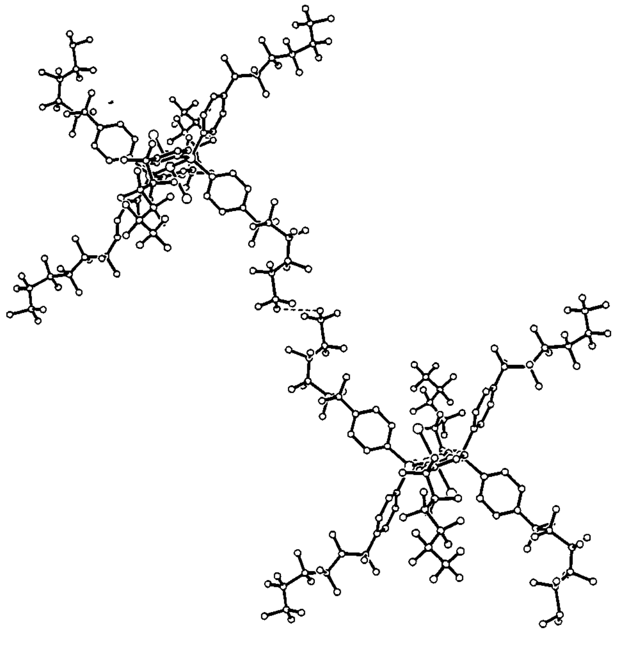

Fig. 6 Unusual interactions between the unique perfluoroalkyl chains in *trans*-[PtCl$_2${P(C$_6$H$_4$C$_6$F$_{13}$-4)$_3$}$_2$].

Kinetic studies

An alternative way to assess the influence of ligands is to study the reactions of the metal complexes. Here, we have, initially, chosen to use the well established rate of O$_2$ addition to the [IrCl(CO)L$_2$] **7**–**9** complexes as a probe.[45] For comparison purposes we have also investigated the rates for the analogous PPh$_3$ and P(C$_6$H$_4$CF$_3$-4)$_3$ **10** complexes under the same conditions. In these studies we have examined the variation in substrate/product concentrations using IR spectroscopy in the carbonyl stretching region and have chosen chloroform as the solvent. This is not ideal since the solubility of oxygen in CHCl$_3$ is relatively low, but it is the only solvent in which all the complexes would dissolve at a high enough concentration to offer accurate analysis of the data. Two experimental methods have been adopted (Experimental section). In the first the well established pseudo-first-order kinetics for this oxidation has been created by bubbling oxygen through an oxygen-saturated solution of the metal complex throughout the experiment. The results (Fig. 8) indicate a sequential drop in the rate of oxidation with the stepwise introduction of pairs of ponytails. The half-lives are calculated to be PPh$_3$ 62 min (which is comparable to that observed previously[45]), PPh$_2$(C$_6$H$_4$C$_6$F$_{13}$-4) 132 min, PPh(C$_6$H$_4$C$_6$F$_{13}$-4)$_2$ 380 min, P(C$_6$H$_4$C$_6$F$_{13}$-4)$_3$ 1395 min and P(C$_6$H$_4$CF$_3$-4)$_3$ 980 min. A comparable drop in reaction rate has been reported between *trans*-[IrCl(CO)(PPh$_3$)$_2$] and *trans*-[IrCl(CO){P(C$_2$H$_4$C$_6$F$_{13}$)$_3$}$_2$] from NMR studies in THF solution.[20] At first glance it is tempting to attribute this variation

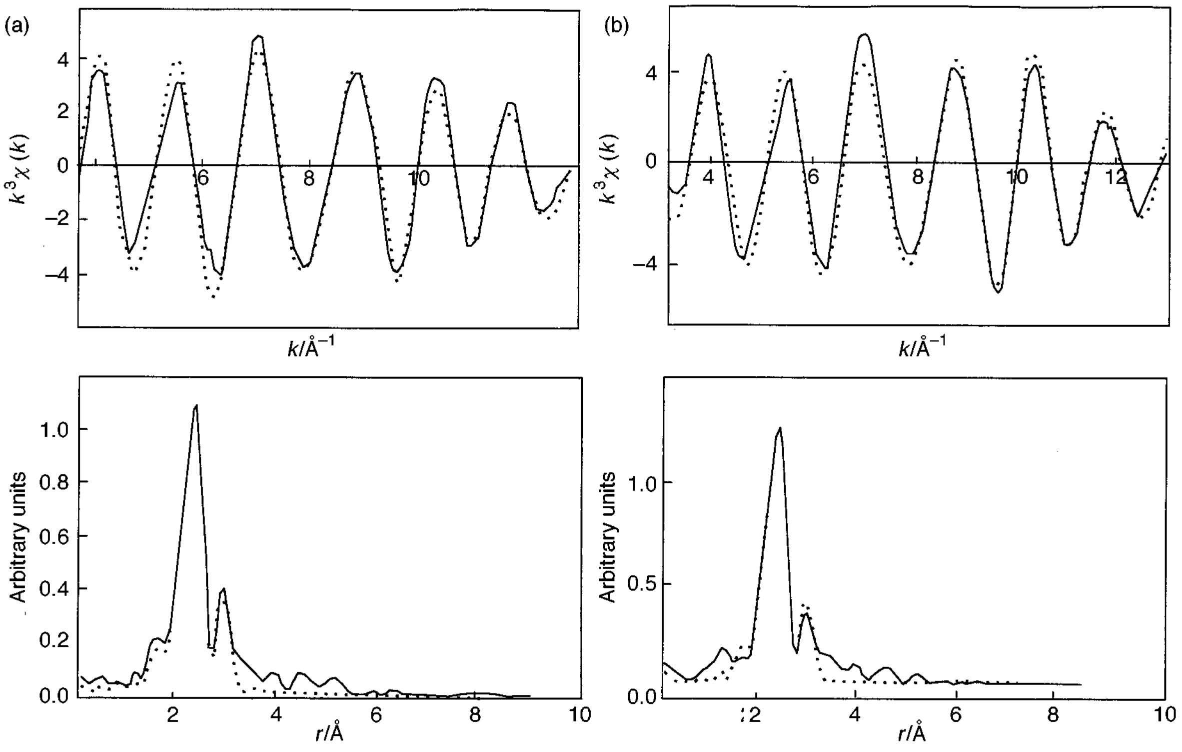

Fig. 7 Background-subtracted EXAFS (——, experimental × k^3; ----, curved-wave theory × k^3) and the Fourier transform (——, experimental; ----, theoretical) for (a) *trans*-[IrCl(CO)(PPh$_3$)$_2$] and (b) *trans*-[IrCl(CO){P(C$_6$H$_4$C$_6$F$_{13}$-4)$_3$}$_2$]; k is the photoelectron wave vector and r is the radial distance from the absorbing atom.

Table 7 Rhodium and palladium K-edge and iridium and platinum L_{III}-edge EXAFS data for model compounds[a]

Complex	d(M–C)[b]/Å	d(M–C)/Å	$2\sigma^2$[c]/Å^2	d(M–P)[b]/Å	d(M–P)/Å	$2\sigma^2$[c]/Å^2	d(M–Cl)[b]/Å	d(M–Cl)/Å	$2\sigma^2$[c]/Å^2	d(M···O)[b]/Å	d(M···O)/Å	$2\sigma^2$[c]/Å^2	EF[d]	F.I.[e]	R[f]
trans-[RhCl(CO)L_2][g]	1.807(5)	1.799(3)	0.001(1)	2.302(1)	2.326(2)[h]	0.008(1)	2.356(2)	—	—	2.959	2.928(4)	0.004(1)	−1.75(32)	3.17	22.11
trans-[IrCl(CO)L_2][i]	1.791(13)	1.791(5)	0.004(1)	2.330(1)	2.337(2)[h]	0.008(1)	2.382(3)	—	—	2.952	2.937(5)	0.004(1)	−9.29(40)	5.22	21.02
trans-[PdCl_2L_2][j]	—	—	—	2.337	2.373(4)	0.003(1)	2.290	2.272(3)	0.003(1)	—	—	—	−2.72(30)	1.04	13.37
cis-[PtCl_2L_2][k]	—	—	—	2.258	2.269(3)	0.004(1)	2.345	2.362(2)	0.003(1)	—	—	—	−11.51(42)	3.57	23.82

[a] Standard deviations in parentheses. The systematic errors in bond distances arising from the data collection and analysis procedures are *ca.* ±0.02 Å for the first co-ordination shells and *ca.* ±0.04 Å for subsequent shells. [b] Distance taken from crystallographic studies. [c] Debye–Waller factor. [d] Fermi energy. [e] Fit Index = $\Sigma_i[(\chi^T - \chi^E)k_i^3]^2$. [f] $R = [\int(\chi^T - \chi^E)k^3dk/\int\chi^E k^3dk] \times 100\%$. [g] L = $P(C_2H_4C_6F_{13})_3$; Crystallographic data taken from ref. 29. [h] M–P and M–Cl modelled to a single shell of 3 × P atoms (see text). [i] L = PPh_3; crystallographic data taken from ref. 40. [j] L = PPh_3; crystallographic data taaken from ref. 41. [k] L = PPh_3; crystallographic data taken from ref. 37.

Table 8 Rhodium and palladium K-edge and iridium and platinum L_{III}-edge EXAFS data for complexes **4**–**14**[a]

Complex	d(M–C)/Å	$2\sigma^2$/Å^2	d(M–P)/Å	$2\sigma^2$/Å^2	d(M–Cl)/Å	$2\sigma^2$/Å^2	d(M···O)/Å	$2\sigma^2$/Å^2	EF	F.I.	R
4	1.806(3)	0.002(1)	2.346(2)	0.009(1)	—	—	2.932(4)	0.006(1)	−0.42(29)	2.60	18.42
5	1.825(4)	0.002(1)	2.348(2)	0.005(1)	—	—	2.952(4)	0.006(1)	−1.82(43)	2.91	19.90
6	1.813(3)	0.001(1)	2.343(2)	0.010(1)	—	—	2.944(14)	0.009(1)	−1.32(37)	2.62	17.98
7	1.802(6)	0.013(1)	2.343(1)	0.009(1)	—	—	2.934(2)	0.001(1)	−7.55(24)	2.80	20.45
8	1.820(5)	0.004(1)	2.338(1)	0.006(1)	—	—	2.944(5)	0.004(1)	−8.76(26)	3.45	22.16
9	1.816(5)	0.002(1)	2.337(2)	0.006(1)	—	—	2.944(5)	0.004(1)	−9.26(34)	3.31	22.19
10	—	—	2.370(3)	0.001(1)	2.259(3)	0.002(1)	—	—	−2.05(34)	1.12	13.76
11	—	—	2.362(5)	0.003(1)	2.270(3)	0.003(1)	—	—	−3.63(32)	0.84	10.90
12	—	—	2.359(4)	0.002(1)	2.261(3)	0.002(1)	—	—	−4.21(33)	0.93	11.47
13	—	—	2.268(5)	0.006(1)	2.350(5)	0.006(1)	—	—	−13.66(44)	3.18	22.87
14	—	—	2.281(6)	0.006(1)	2.342(4)	0.008(2)	—	—	−13.95(62)	2.50	19.48

[a] Details as in Table 7.

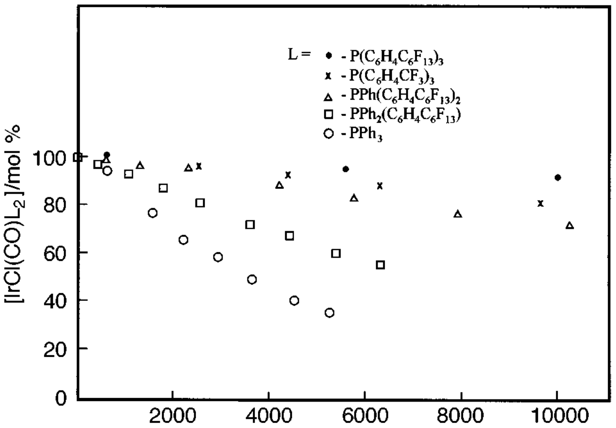

Fig. 8 Rates of reaction of *trans*-[IrCl(CO)L_2] (2.566 mM) and O_2 (8.52 mM) in $CHCl_3$ at room temperature.

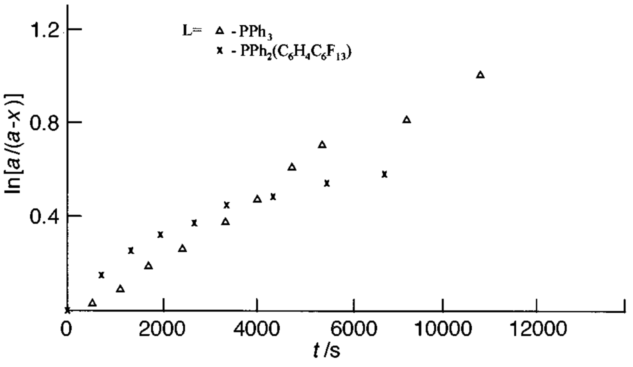

Fig. 9 Plots of ln [a/(a − x)] *vs.* time for the reactions of *trans*-[IrCl(CO)L_2] [L = PPh_3 or $PPh_2(C_6H_4C_6F_{13}$-4); 0.436 mM] and O_2 (8.710 mM) in $CHCl_3$ at room temperature.

solely to the electronic influence of the perfluoroalkyl substituents. However, the spectroscopic and structural data (see above) suggest that the introduction of the ponytails in these aryl ligands has a limited effect; the IR data for [IrCl(CO)(O_2){P(C_6H_4-C_6F_{13}-4)$_3$}$_2$] [(ν(CO) 2025 and ν(O–O) 861 cm^{-1})] are very similar to those for the PPh_3 complex (2015 and 858 cm^{-1} respectively).[46] In an attempt to confirm that these reactions are genuinely pseudo-first-order a second set of experiments were undertaken (method 2). Here, the rates of reaction were investigated at fixed (closed-system) excess oxygen concentrations (20:1, 15:1 and 10:1). For the triphenylphosphine complex the well established pseudo-first-order kinetics was confirmed under our conditions and the calculated second order rate constant (0.02 M^{-1} s^{-1} in chloroform at 23 °C) is similar to that calculated previously.[47] However, the introduction of only two ponytails under this experimental set-up had an enormous effect on the rate of oxidation. In contrast to the results obtained under method 1, 50% conversion was only reached after *ca.* 24 h (*cf.* $t_{\frac{1}{2}} = 132$ min) and analysis did not reveal pseudo-first-order kinetics (Fig. 9). For the tris-derivatised ligand metal complex this decelaration was multiplied several fold. These results indicate that in these closed systems, even at a 20:1 O_2:complex ratio, there is insufficient oxygen to maintain pseudo-first-order kinetics. It is also unlikely that pseudo-first-order kinetics was established in the earlier study[20] where the O_2:complex ratio was only 3:1. These results suggest that for the fluorous-derivatised metal complexes there is an additional "reaction" and we believe that this may offer an additional explanation for the relative reaction rates illustrated in Fig. 8. It is well known that high concentrations of oxygen dissolve in perfluorocarbon solvents and that this occurs by trapping the oxygen molecules in voids in the solvent structure.[48] Guillevic *et al.*[20] have shown that the rate of O_2 addition to *trans*-[IrCl(CO){P($C_2H_4C_6F_{13}$)$_3$}$_2$] is very much slower in perfluoromethylcyclohexane than in THF, which they have ascribed to the high affinity of the solvent for the oxygen molecules. We have noted that it is very difficult to remove dissolved oxygen from our ligands in solution, and we believe that the ponytails on our ligands and metal complexes have an affinity for small molecules which may be similar to that for the perfluorocarbon solvents. Consequently, during these kinetic studies there is an alternative interaction whereby the oxygen molecules interact strongly with the perfluoroalkyl chains decreasing the apparent oxygen concentration in solution. Further kinetic and physical studies are necessary in this area to establish the exact nature of any interaction and the role of the fluorous ponytails in reactions at metal centres.

Solubility studies

The value of the FBS approach to catalysis depends upon the partition of the metal complex/catalyst in a two-phase organic/fluorous solvent system. In this study at least six ponytails per metal centre are required to make a metal complex preferentially soluble in a perfluorocarbon solvent as shown by the complete absence of signals in the ^{31}P-{^{1}H} NMR spectra of the toluene phases after shaking these complexes in a toluene–PP3 two-phase system. At this six ponytail limit the type of metal complex appears to be important *i.e.* *trans*-[MCl(CO)L_2] (M = Rh or Ir) are preferentially PP3 soluble whilst *cis*- and *trans*-[MCl_2L_2] (M = Pd or Pt) are not. Increasing the number of ponytails to nine, for example in [RhClL_3], gives metal complexes which are very perfluorocarbon solvent soluble and difficult to isolate except as very viscous oils. The NMR spectra†

---

† ^{31}P-{^{1}H} NMR data for [RhCl{$PPh_{3-x}(C_6H_4C_6F_{13}$-4)$_x$}]. $x = 0$ (CH_2Cl_2): δ 31.5 (2P, dd $^1J_{RhP}$ 142, $^2J_{PP}$ 38, $P_{trans\text{-}P}$) and 48.0 (1P, dt, $^1J_{RhP}$ 193, $^2J_{PP}$ 38 Hz, $P_{cis\text{-}P}$).[49] $x = 1$ ($CDCl_3$): δ 31.0 (2P, dd, $^1J_{RhP}$ 143, $^2J_{PP}$ 38, $P_{trans\text{-}P}$) and 47.8 (1P, dt, $^1J_{RhP}$ 193, $^2J_{PP}$ 38 Hz, $P_{cis\text{-}P}$). $x = 3$ (PP3): δ 31.5 (2P, dd, $^1J_{RhP}$ 144, $^2J_{PP}$ 37, $P_{trans\text{-}P}$) and 48.0 (1P, dt, $^1J_{RhP}$ 190, $^2J_{PP}$ 37 Hz, $P_{cis\text{-}P}$).

for these complexes confirm the presence of three ligands at the metal centre, but we have been unable to obtain further characterisation data for these derivatives.

Conclusion

The reactions of ligands with perfluoroalkyl ponytails with platinum group metal starting materials readily affords metal complexes of these ligands either by cleavage of chloride bridges or by displacement of weakly co-ordinating ligands. Spectroscopic and structural studies indicate that the introduction of the ponytails reduces the σ-donor strength of the ligands but this is compensated by π effects resulting in little overall affect on the metal co-ordination environment. Solubility studies indicate that at least six ponytails are required for preferential solubility in perfluorinated solvents. However, increasing the number of ponytails can afford complexes which are difficult to isolate in a pure form as a consequence of the number of perfluoroalkyl substituents. Preliminary kinetic studies on the reaction of oxygen with analogues of Vaska's complex indicate that the oxidation is not as straightforward as that described for complexes without perfluoroalkyl substituents and further work on this aspect of this work is underway.

Acknowledgements

We would like to thank the Royal Society (E. G. H.), the EPSRC (D. R. P., A. M. S.) and BP Chemicals Ltd. (D. R. P.) for financial support, Dr G. Eaton for recording the mass spectral data, the EPSRC X-ray crystallography service for data collection for complex **3**, the Director of the Daresbury laboratory for the provision of facilities, Dr M. Jones (BP Chemicals Ltd.) for helpful discussions and Drs J. Burgess and E. Raven (*née* Lloyd) for assistance with the kinetic studies.

References

1 I. T. Horváth and J. Rábai, *Science*, 1994, **266**, 72; *US Pat.*, 5 463 082, 1995.
2 J. J. J. Juliette, I. T. Horváth and J. A. Gladysz, *Angew. Chem.*, *Int. Ed. Engl.*, 1997, **36**, 1610.
3 I. Klement, H. Lütjens and P. Knochel, *Angew. Chem.*, *Int. Ed. Engl.*, 1997, **36**, 1454; J. M. Vincent, A. Rabion, V. K. Yachandra and R. H. Fish, *Angew. Chem.*, *Int. Ed. Engl.*, 1997, **36**, 2346.
4 D. P. Curran and S. Hadida, *J. Am. Chem. Soc.*, 1996, **118**, 2531; D. P. Curran and M. Hoshino, *J. Org. Chem.*, 1996, **61**, 6480; A. Studer and D. P. Curran, *Tetrahedron*, 1997, **53**, 6681; A. Studer, S. Hadida, R. Ferritto, S. Y. Kim, P. Jeger, P. Wipf and D. P. Curran, *Science*, 1997, **275**, 823.
5 B. Betzemeier and P. Knochel, *Angew. Chem.*, *Int. Ed. Engl.*, 1997, **36**, 2623.
6 G. Pozzi, S. Banfi, A. Manfredi, F. Montanari and S. Quici, *Tetrahedron*, 1996, **52**, 11879; G. Pozzi, F. Montanari and S. Quici, *Chem. Commun.*, 1997, 69; G. Pozzi, I. Colombani, M. Miglioli, F. Montanari and S. Quici, *Tetrahedron*, 1997, **53**, 6145; G. Pozzi, F. Cinato, F. Montanari and S. Quici, *Chem. Commun.*, 1998, 877.
7 P. Bhattacharyya, D. Gudmunsen, E. G. Hope, R. D. W. Kemmitt, D. R. Paige and A. M. Stuart, *J. Chem. Soc.*, *Perkin Trans. 1*, 1997, 3609.
8 A. K. Brisdon, EX, A Program for EXAFS Data Reduction, University of Leicester, 1992.
9 N. Binsted, S. J. Gurman and J. W. Campbell, EXCURV 92, SERC Daresbury Laboratory Program, 1992.
10 S. J. Gurman, N. Binsted and I. Ross, EXCURVE, *J. Phys. C*, 1984, **17**, 143; 1986, **19**, 1845.
11 F. R. Hartley, S. G. Murray and C. A. McAuliffe, *Inorg. Chem.*, 1979, **18**, 1394.
12 J. Herde, J. C. Lambert and C. V. Senoff, *Inorg. Synth.*, 1974, **15**, 18.
13 R. J. Goodfellow and L. M. Venanzi, *J. Chem. Soc.*, 1965, 7533.
14 *Solubilities of Inorganic and Metal Organic Compounds*, 3rd edn., ed. A. Seidell, D. Van Nostrand, New York, 1940, vol. 1, p. 1359.
15 S. R. Davies, M. C. Mitchell, C. P. Cain, P. G. Devitt, R. J. Taylor and T. P. Kee, *J. Organomet. Chem.*, 1998, **550**, 29.
16 M. A. Guillevic, A. M. Arif, I. Horváth and J. A. Gladysz, *Angew. Chem.*, *Int. Ed. Engl.*, 1997, **36**, 1612.
17 F. R. Hartley, *The Chemistry of Platinum and Palladium*, Applied Science, London, 1973, p. 456.
18 K. G. Moloy and J. L. Peterson, *J. Am. Chem. Soc.*, 1995, **117**, 7696.
19 K. Vrieze, J. P. Collman, C. T. Sears and M. Kubota, *Inorg. Synth.*, 1968, **11**, 101.
20 M. A. Guillevic, C. Rocaboy, A. M. Arif, I. T. Horváth and J. A. Gladysz, *Organometallics*, 1998, **17**, 707.
21 A. J. Deeming and B. L. Shaw, *J. Chem. Soc. A*, 1968, 1887.
22 M. J. Atherton, J. Fawcett, A. P. Hill, J. H. Holloway, E. G. Hope, D. R. Russell, G. C. Saunders and R. M. J. Stead, *J. Chem. Soc.*, *Dalton Trans.*, 1997, 1137.
23 A. F. Williams, S. Bhaduri and A. G. Maddock, *J. Chem. Soc.*, *Dalton Trans.*, 1975, 1958.
24 J. J. MacDougall and J. H. Nelson, *Inorg. Nucl. Chem. Lett.*, 1979, **15**, 315.
25 R. G. Goel, *Inorg. Nucl. Chem. Lett.*, 1979, **15**, 437.
26 C. J. Cobley and P. G. Pringle, *Inorg. Chim. Acta.*, 1997, **265**, 107.
27 J. March, *Advanced Organic Chemistry*, Wiley, New York, 4th edn., 1992, p. 280.
28 A. Crispini, K. N. Harrison, A. G. Orpen, P. G. Pringle and J. R. Wheatcroft, *J. Chem. Soc.*, *Dalton Trans.*, 1996, 1069 and refs. therein.
29 J. Fawcett, E. G. Hope, R. D. W. Kemmitt, D. R. Paige, D. R. Russell, A. M. Stuart, D. J. Cole-Hamilton and M. J. Payne, *Chem. Commun.*, 1997, 1127.
30 B. Albinsson and J. Michl, *J. Phys. Chem.*, 1996, **100**, 3418.
31 L. Xue, D. D. DesMarteau and W. T. Pennington, *Angew. Chem.*, *Int. Ed. Engl.*, 1997, **36**, 1331.
32 C. R. Jablonski and Z. Zhou, *Can. J. Chem.*, 1992, **70**, 2544.
33 P. Kromm, J. -P. Bideau, M. Cotrait, C. Destrade and H. Nguyen, *Acta Crystallogr.*, *Sect. C*, 1994, **50**, 112.
34 R. D. Brost, G. C. Bruce, S. L. Grundy and S. R. Stobart, *Inorg. Chem.*, 1993, **32**, 5195.
35 W. Keim, P. Kraneburg, G. Dahmen, G. Deckers, U. Englert, K. Linn, T. P. Spaniol, G. Raabe and C. Kruger, *Organometallics*, 1994, **13**, 3085.
36 S. Ogo, T. Suzuki, Y. Ozawa and K. Isobe, *Inorg. Chem.*, 1996, **35**, 6093.
37 G. K. Anderson, H. C. Clark, J. A. Davies, G. Ferguson and M. Parvez, *J. Crystallogr. Spectrosc. Res.*, 1982, **12**, 449.
38 A. G. Orpen, L. Brammer, F. H. Allen, O. Kennard, D. G. Watson and R. Taylor, *J. Chem. Soc.*, *Dalton Trans.*, 1989, S1.
39 M. J. Atherton, K. S. Coleman, J. Fawcett, J. H. Holloway, E. G. Hope, A. Karaçar, L. A. Peck and G. C. Saunders, *J. Chem. Soc.*, *Dalton Trans.*, 1995, 4029; H. C. S. Clark, J. Fawcett, J. H. Holloway, E. G. Hope, L. A. Peck and D. R. Russell, *J. Chem. Soc.*, *Dalton Trans.*, 1998, 1249.
40 M. R. Churchill, J. C. Fettinger, L. A. Buttrey, M. D. Barkan and J. S. Thompson, *J. Organomet. Chem.*, 1988, **340**, 257.
41 G. Ferguson, R. McCrindle, A. J. McAlees and M. Parvez, *Acta Crystallogr., Sect. B*, 1982, **38**, 2679.
42 R. W. Joyner, K. J. Martin and P. Meehan, *J. Phys. C*, 1987, **20**, 4005.
43 N. Binsted, S. L. Cook, J. Evans, G. N. Greaves and R. J. Price, *J. Am. Chem. Soc.*, 1987, **109**, 3669.
44 See, for example, N. R. Champness, W. Levason, D. Pletcher, M. D. Spicer and M. Webster, *J. Chem. Soc.*, *Dalton Trans.*, 1992, 2201.
45 C. A. McAuliffe and R. Pollock, *J. Organomet. Chem.*, 1974, **77**, 265.
46 P. B. Chock and J. Halpern, *J. Am. Chem. Soc.*, 1966, **88**, 3511.
47 H. Stieger and H. Kelm, *J. Phys. Chem.*, 1973, **77**, 290.
48 J. G. Riess and M. LeBlanc, *Pure Appl. Chem.*, 1982, **54**, 2383.
49 T. H. Brown and P. J. Green, *J. Am. Chem. Soc.*, 1970, **92**, 2359.

Paper 8/05141K